Bulgarian Chemical Communications, Volume 47, Number 2 (pp. 587 – 593) 2015

Synthesis and characterization of Si and Mg substituted lithium vanadium(III) phosphate

S. M. Stankov[1]*, A. Momchilov[1], I. Abrahams[2], I. Popov[1], T. Stankulov[1], A. Trifonova[3]

[1]*Institute of Electrochemistry and Energy Systems "Acad. Evgeni Budevski", Bulgarian Academy of Sciences, Acad. Georgi Bonchev Str., Block 10, 1113 Sofia, Bulgaria.*

[2] *Materials Research Institute, School of Biological and Chemical Sciences, Queen Mary University of London, Mile End Road, London E1 4NS, United Kingdom.*

[3] *AIT Austrian Institute of Technology GmbH, Giefinggasse 2, 1210 Vienna, Austria.*

Received May 12, 2014, Revised July 15, 2014

Active materials for lithium ion batteries based on Si and Mg substitution in lithium vanadium(III) phosphate, $Li_3V_2(PO_4)_3$ (LVP), were investigated using X-ray powder diffraction, thermal analysis, transmission electron microscopy, galvanostatic tests and cyclic voltammetry. $Li_3V_2(PO_4)_3$, $Li_{3.1}V_2(SiO_4)_{0.1}(PO_4)_{2.9}$, $Li_{3.5}V_2(SiO_4)_{0.5}(PO_4)_{2.5}$ and $Li_{3.04}Mg_{0.03}V_2(SiO_4)_{0.1}(PO_4)_{2.9}$ were prepared as carbon coated powders, through wet chemistry (sol-gel) followed by solid state routes under Ar. X-ray powder diffraction confirmed that the basic monoclinic structure of LVP was preserved in the substituted systems. Electrochemical testing on two electrode cells based on these materials at a charge-discharge rate of 0.2C in the range 2.8-4.4 V showed that the Mg substituted system delivers the highest discharge capacity of 124.8 mA h g^{-1}, achieving 94% of its theoretical capacity (133 mA h g^{-1}) in this voltage range. However, this material shows poor long-term cycling behavior, with approximately 20% capacity fade over 100 cycles. Generally it is found that Si substitution has a negative effect on initial capacity, but following a capacity fade of up to 15% in the first 15 cycles, the Si substituted systems show nearly constant capacity on further cycling.

Keywords: Lithium Vanadium Phosphate, Positive Active Material, Li-ion Battery

INTRODUCTION

Lithium-ion battery (LIB) technology has developed over the past two decades, due to the high energy density and output voltage of systems based on this technology. Cathode specific capacity is a limiting factor in LIBs, particularly for transport applications, so high energy density materials are being searched for. Lithium cobalt oxide, $LiCoO_2$ [1], is the most commonly used positive active material in the industry, but there are issues related to the environment and health care, as well as cost, which limit its widespread use for transport applications. Other layered oxides like $Li(Ni_{1/3}Co_{1/3}Mn_{1/3})O_2$ [2] and $LiMn_2O_4$ [3] have also found places in the market. Materials based on phosphate polyanions are very attractive because of their relatively high energy density, non-toxicity and inexpensiveness. $LiFePO_4$ [4] has already successfully been implemented in the industry and other phosphate and fluorophosphate materials such as $Li_3V_2(PO_4)_3$ [5], $LiMnPO_4$ [6], $LiCoPO_4$ [7], $LiNiPO_4$ [8], $LiVPO_4F$ [9], *etc*. are being considered for the next generation of commercial materials. The main drawbacks of these materials are low electronic and ionic conductivity and instability during operation [10-11]. Although the problem of low electronic conductivity has been addressed for some of these materials by applying so-called carbon coating [12-14], other issues like short cycle-life remain.

Among the above mentioned phosphates, $Li_3V_2(PO_4)_3$ (LVP) has the highest theoretical specific capacity of 197 mA h g^{-1} for removal of three moles of lithium per mole of LVP. Studies have confirmed de-intercalation at high potentials, with four characteristic plateaus *versus* Li/Li^+ at 3.6 and 3.68 V, corresponding to the first Li extraction, 4.2 V and over 4.5 V, corresponding to the second and third lithium extractions, respectively [15]. Due to structural instability at high potentials, with consequent rapid decline in discharge capacity, studies have focused on a more limited operational voltage range of 3.0 to 4.4 V [16-17]. In this voltage range, the theoretical specific capacity is ~131.5 mA h g^{-1} for two moles of lithium per mole LVP. To overcome the structural instability obstacle at high potentials, many groups have researched the effect of doping on LVP. Different elements like Cr, Mo, Y, Al, *etc*. [18-21] can partially replace vanadium, while oxygen in the phosphate group can be partially substituted by chlorine [21].

* To whom all correspondence should be sent:
E-mail: s.stankov@mail.bg

The aim of the present study was to investigate the effects of substitution of silicon for phosphorus in lithium vanadium phosphate on structure and electrochemical performance. Silicon and phosphorus show similar structural chemistry, adopting tetrahedral geometry in oxide systems, forming $(SiO_4)^{4-}$ and $(PO_4)^{3-}$, respectively. Two methods of charge balance are investigated in the system: (i) through additional Li^+ and (ii) through addition of Mg^{2+}.

EXPERIMENTAL

Preparations

Carbon coated samples of $Li_3V_2(PO_4)_3$ (LVPC), $Li_{3.1}V_2(SiO_4)_{0.1}(PO_4)_{2.9}$ (LVS10PC), $Li_{3.5}V_2(SiO_4)_{0.5}(PO_4)_{2.5}$ (LVS50PC) and $Li_{3.04}Mg_{0.03}V_2(SiO_4)_{0.1}(PO_4)_{2.9}$ (LMgVSPC) were synthesized *via* a three-step sol-gel method. Stoichiometric amounts of V_2O_5 (synthesized by decomposition of NH_4VO_3, Fluka, >99% at 320°C), and $H_2C_2O_4.2H_2O$ (Sigma-Aldrich, ≥98.5%) were dissolved in distilled water to give a blue-green solution. To this were added separate solutions of stoichiometric amounts of $LiOH.H_2O$ (Sigma-Aldrich, ≥98%) and $(NH_4)H_2PO_4$ (Sigma-Aldrich, ≥98%) dissolved in distilled water. Colloidal silica (Silica sol, $mSiO_2.nH_2O$, Qingdao YuKai Import and Export Co.,Ltd) with SiO_2 30-31 wt% in solution, an average particle size of 10-20 nm and pH=8.5-10, was added to the mixture for LVS10PC, LVS50PC and LMgVSPC samples. $MgCl_2.6H_2O$ (Merck, >98%) was employed as the magnesium precursor for the LMgVSPC material. Glycine (NH_2CH_2COOH, Sigma-Aldrich, ≥ 98.5 %) was used as a carbon source for all samples. For the LVPC sample acetylene black P1042 (AB) [22] was added to the mixture as an additional carbon source, as well as 1 to 2 drops of Triton X-100, which served as a surfactant for decreasing the surface tension around suspended AB particles. The final solution was evaporated with constant stirring at 80 °C for *ca.* 4 h until it became a gel. The gel was dried in an oven at 120 °C for 16 h and the resulting powder was heated at 370 °C for 4 h in Ar flow in order to remove ammonia and water. The intermediate precursor was ground for 30 min and then annealed at 800 °C for 10 h under Ar.

Sample characterization

X-ray powder diffraction (XRD) data were collected on a PANalyticalX'Pert Pro diffractometer fitted with an X'Celerator detector, using Ni-filtered Cu-Kα radiation (λ = 1.5418 Å), over the 2θ range 5-120°, with a step width of 0.033° and an effective scan time of 200 s per step at room temperature. Data were modeled by Rietveld analysis using the GSAS suite of programmers [23]. The structures of $Li_3V_2(PO_4)_3$ (with appropriate substitution of Si for P) [24], Li_3PO_4 [25] and VO [26], were used as starting models in the refinements. Thermogravimetric and differential thermal analyses were carried out for the LVPC precursor in Ar, on a Stanton Redcroft thermogravimetric analyzer in the range 20-760 °C, with a heating rate of 5 °C per min. Transmission electron microscopy (TEM) was carried out on a JEOL JEM 2010 microscope, with an accelerating voltage of 200 kV and a beam current of 106 μA.

Electrochemical testing

The obtained materials were electrochemically tested in two-electrode laboratory cells. The working electrodes were prepared by mixing active material (AM), PVDF (MTI corp., USA) and acetylene black (AB) P1042 in N-methyl-2-pyrrolidone (NMP, MTI corp., USA). The ratio of the slurry was AM:PVDF 70:10 wt.%, with acetylene black and the carbon coating of the active material constituting the remaining 20 wt.%. The slurries were stirred for 24 h and then coated onto aluminum foil. The coated foils were dried under vacuum at 120°C for 24 h. Cells were assembled using lithium foil (Alfa Aesar) as the counter electrode, with Freudenberg FS 2190 as a separator. The electrolyte used was 1M $LiClO_4$ (Alfa Aesar) in a 1:1 (v/v) mixture of ethylene carbonate (EC) and dimethyl carbonate (DMC) (both purchased from Alfa Aesar). Electrochemical galvanostatic tests were performed on a Neware Battery Testing System (V-BTS8-3), in the voltage range 2.8 - 4.4 V for all four materials and 2.8 - 4.8 V only for LVPC, at a C/5 (0.2C) rate, where C is the theoretical specific capacity for 3 moles of extracted Li, *i.e.* 197 mA h g^{-1} and 5 is the charge or discharge time in hours. Cyclic voltammetry (CV) was performed on a VersaSTAT MC (Princeton Applied Research) multi-channel potentiostat/ galvanostat, with a step rate of 20 μV s^{-1}, where the counter Li electrode was also used as a reference, as its polarization is negligible.

RESULTS AND DISCUSSION

Thermogravimetric and differential thermal analyses (Fig. 1) were carried out for the LVPC gel precursor obtained after the first synthesis step. The differential thermogram shows significant endotherms at 131 and 142, 241 and 308 °C. These peaks are associated mostly with loss of water and ammonia which is in agreement with the

thermogravimetric measurement. The major weight loss is 55.5 wt.% in the range 20-388 °C. The exotherms in the range 350-600 °C correspond to the product formation. The weight loss is 12.34% in the range 388-760 °C.

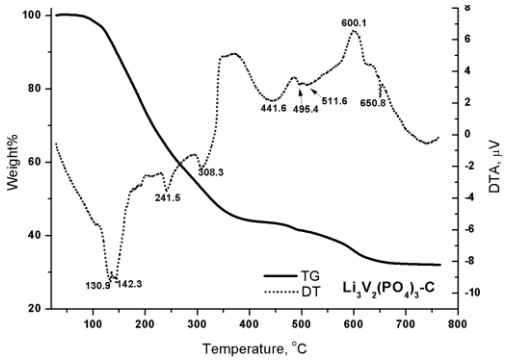

Fig. 1. Thermogravimetric (TG) and differential thermal (DT) analyses of LVPC precursor.

The X-ray powder diffraction data (Fig. 2) are similar and show a monoclinic $Li_3V_2(PO_4)_3$ type phase, in space group $P2_1/n$. Besides the desired phase, the patterns for LVPC and LVS50PC display peaks corresponding to Li_3PO_4, while LVPC, LVS10PC and LVS50PC additionally show broad peaks from a cubic phase that appears to correspond to VO, suggesting some reduction of the vanadium to V^{2+}. Only LMgVSPC was isolated as a single phase. Table 1 summarizes the refined unit cell parameters and weight fractions obtained through Rietveld analysis of the data. None of the silicate containing samples showed the presence of a separate silicate phase and appeared to confirm successful substitution of Si for P in the main phase. Indeed, the increase in unit cell volume with increasing Si substitution, is consistent with the substitution of P(V) with Si(IV), with respective ionic radii of 0.17 Å and 0.26 Å [27].

Fig. 3 depicts TEM images of the obtained materials. LVPC particles (Fig. 3a) are surrounded by large masses of carbon, most likely acetylene black P1040. LMgVSPC and LVS10PC (Figs. 3b and 3c) samples show the presence of large clusters composed of small particles of active material, which are held together by carbon. LVS50PC (Fig. 3d) displays an uneven distribution of active material and carbon. The particle (agglomerate) size varies from 30 nm to 5 μm for LVPC (with an average in the range 50-300 nm), 0.2-10 μm for LMgVSP, 0.15-7.5 μm for LVS10PC and 0.2-8 μm for LVS50PC.

Second cycle charge-discharge curves for the test cells at a 0.2C rate, in the range 2.8–4.4 V are shown in Fig. 4. All curves show the characteristic three charge-discharge plateaus, corresponding to the three types of reversible phase transformation in $Li_{3-x}V_2(PO_4)_3$ (x = 0, 0.5, 1.0, and 2.0) [15]. LMgVSPC delivers the highest discharge capacity of 124.8 mA h g^{-1}, achieving 94% of its theoretical capacity (133 mA h g^{-1}) in this voltage range. LVPC, LVS10PC and LVS50PC present discharge capacities of 116.5, 112.6 and 97.8 mA h g^{-1}, respectively. It is notable that increasing amount of Si appears to have a negative effect on the initial capacity, apart from LMgVSPC. For LVS10PC and LVS50PC the discharge profile below 3.5 V is not as steep compared to those of LVPC and LMgVSPC and is indicative of slower kinetics of ion diffusion in these samples.

The cycling performance of the test cells is shown in Fig. 5. LVPC shows a first specific discharge capacity of 118 mA h g^{-1} and relatively good stability, with a capacity decline of 6.7% over 100 cycles and a coulombic efficiency of around 98%.

Table 1. Refined cell dimensions of primary LVP type phase and weight fractions from Rietveld analysis of the studied materials.

Parameter	LVPC	LMgVSPC	LVS10PC	LVS50PC
Wtfrac. 1° phase	0.860(1)	1.00	0.9518(4)	0.731(2)
Wtfrac. Li_3PO_4	0.099(2)			0.19(3)
Wtfrac. VO	0.041(2)		0.048(1)	0.071(3)
1° phase a (Å)	8.5548(3)	8.6083(3)	8.6060(5)	8.6100(5)
1° phase b (Å)	8.6719(3)	8.5958(3)	8.5915(5)	8.5969(5)
1° phase c (Å)	11.9915(4)	12.0416(4)	12.0394(7)	12.0484(7)
1° phase β (°)	89.890(5)	90.564(2)	90.588(4)	90.569(4)
1° phase Vol. (Å^3)	884.06(6)	890.98(7)	890.1(1)	891.8(1)

Of the four samples, LMgVPC displays the greatest initial capacity of ~125 mA h g^{-1}, but it has poor cyclability.

Although the capacity is higher in the first 60 cycles compared to LVPC, the fading is 20.7% over 100 cycles and the coulombic efficiency varies from 90 to 98%. This result is somewhat surprising, since achieving charge balance through addition of Mg^{2+} ions rather than additional Li^{+} ions yields compounds with lower theoretical discharge capacities. The other two silicate containing samples show similar cycling behavior to each other. In the first cycle, the discharge specific capacity of LVS10PC is 116 mA h g^{-1} and declines to ~100 mA h g^{-1}, up to the 15th cycle, corresponding to a 14% loss. The material becomes stable after the 15th cycle and there is no further capacity loss up to the 60th cycle. The coulombic efficiency is 91-97% for this cell over the first 15 cycles and 97-98% thereafter. LVS50PC displays the lowest initial capacity of 102 mA h g^{-1} of all the test samples. For this cell, the capacity fades 16.8% over the first 15 cycles and then remains stable up to the 100th cycle. The coulombic efficiency is 88-96% up to the 15th cycle then rises to 97-99% up to the 100th cycle.

Cyclic voltammetry was performed on the four studied materials (Fig. 6). It is notable that there are significant differences in the delivered currents, which do not correspond to the delivered capacities in galvanostatic mode in Fig. 4.

This is caused by the differences in the weight of the active material used in the electrodes. All four voltammagrams show oxidation potentials at around 3.62, 3.70, 4.12 and 4.53 V, with those of LMgVSP by 15-20 mV higher.

These peaks are associated with the four stages of Li de-intercalation and the corresponding oxidation of vanadium. The third and fourth peaks in the oxidation curve are replaced by a single broad peak at around 3.8-3.9 V on reduction, reflecting a change in structure following de-intercalation of the third lithium. The last two reduction peaks are at around 3.63 and 3.56 V. The results show that LMgVSPC exhibits a higher polarization (100-250 mV) compared to the other three materials (70-150 mV).

This structural change is confirmed by the galvanostatic charge-discharge curves (Fig. 7) for LVPC, investigated at a rate of 0.2C, in the voltage range 2.8–4.8 V. These clearly show an absence of flat plateaus in the discharge profile following the first charge. The capacities of charge and discharge are 189.6 and 147 mAh g^{-1}, respectively, corresponding to a coulombic efficiency of 77.57%

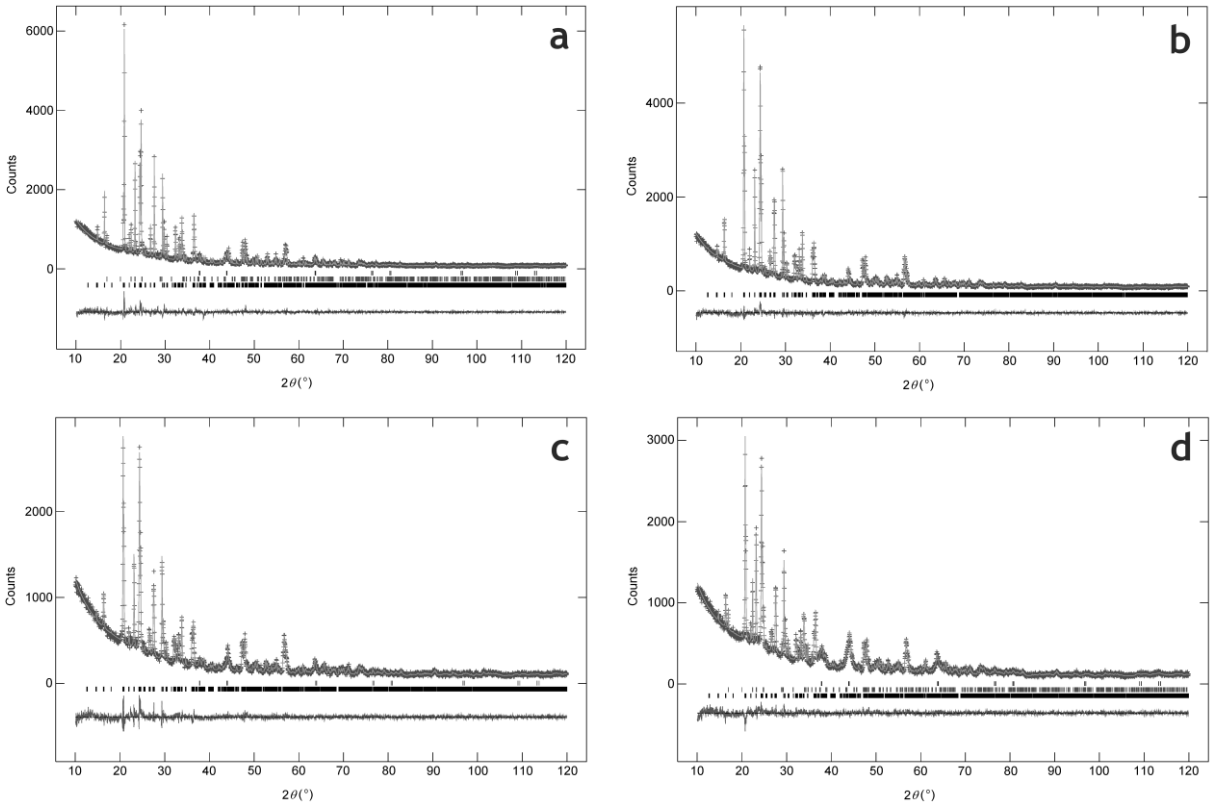

Fig.2. Fitted X-ray diffraction profiles for (a) LVPC, (b) LMgVSPC, (c) LVS10PC and (d) LVS50PC, showing observed (+ symbols), calculated (line), and difference (lower) profiles. Reflection positions are indicated by markers.

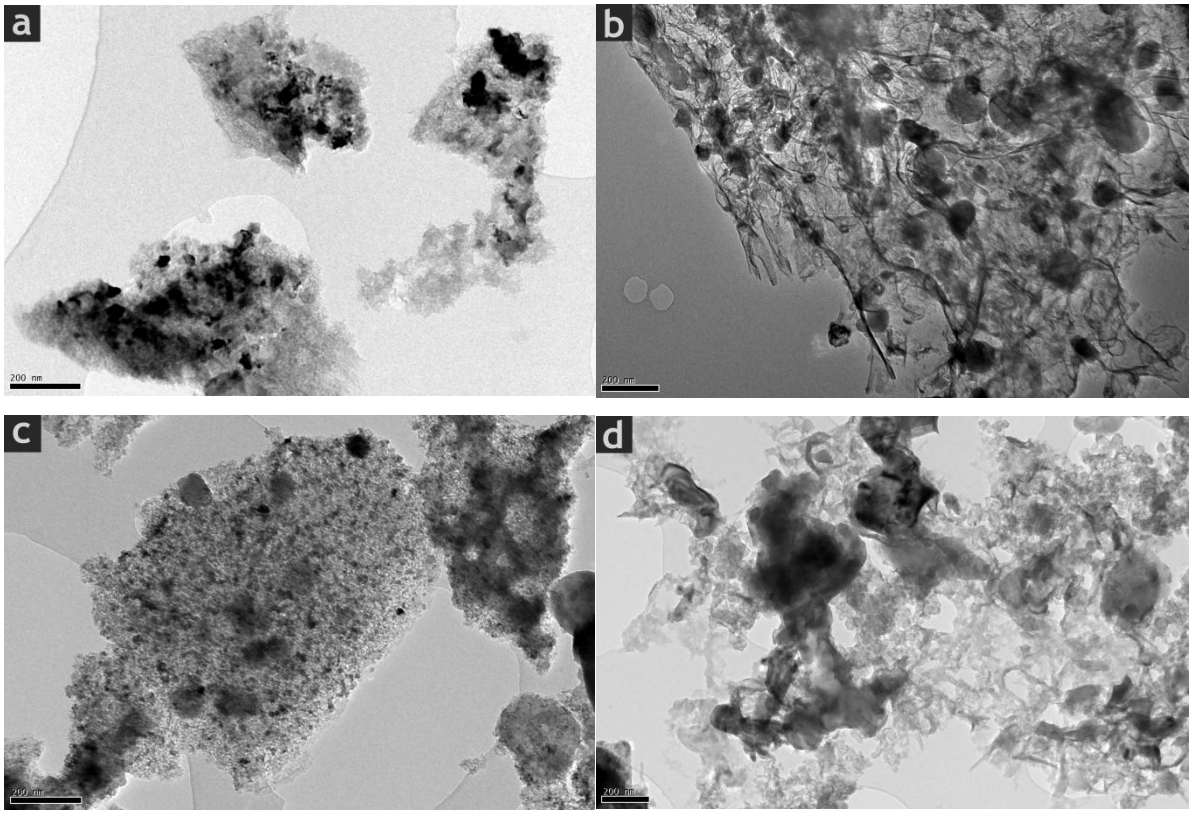

Fig. 3. TEM images of (a) LVPC, (b) LMgVSPC, (c) LVS10PC and (d) LVS50PC.

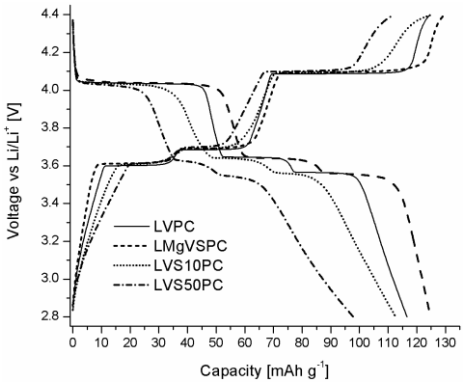

Fig.4. Second cycle charge-discharge profiles of LVPC, LMgVSPC, LVS10PC and LVS50PC at 0.2C rate in the voltage range 2.8-4.4 V *vs*. Li/Li^+.

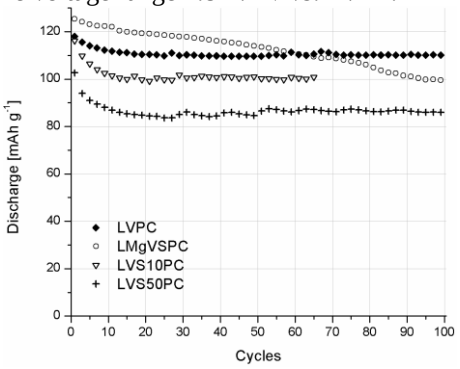

Fig. 5. Discharge capacities of LVPC, LMgVSPC, LVS10PC and LVS50PC recorded during cycling at 0.2C rate in the voltage range 2.8–4.4 V *vs*. Li/Li^+.

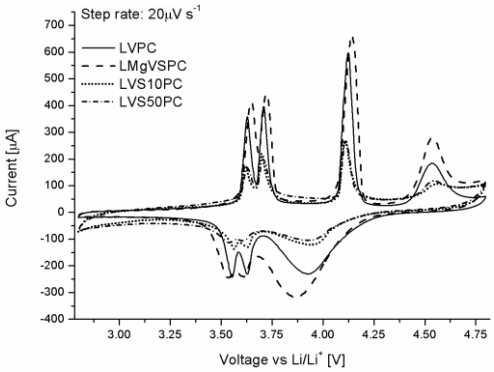

Fig. 6. Cyclic voltammagrams of LVPC, LMgVSPC, LVS10PC and LVS50PC.

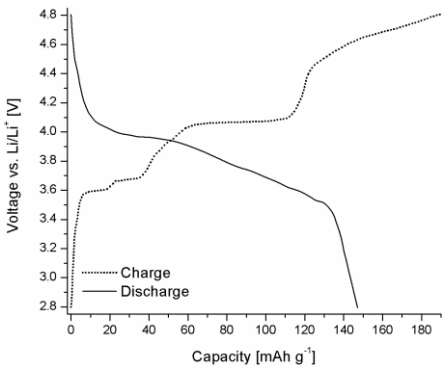

Fig.7. Initial charge-discharge profiles for LVPC at 0.2C rate in the voltage range 2.8-4.8 V *vs*. Li/Li^+.

CONCLUSIONS

Si can successfully be substituted for P in $Li_3V_2(PO_3)_3$. However, Si substitution is found to have a negative effect on initial discharge capacity in cells constructed using these compounds as active material. On cycling, cells using the Si substituted LVP show an initial capacity fade, but after the 15th cycle the capacity remains fairly constant. Inclusion of Mg in this system is found to increase the initial capacity of the Si substituted system, and although cycling behavior is degraded to some extent, the results are encouraging. Studies on the effects of Mg inclusion in isolation warrant further investigation.

Acknowledgements: *This study was supported by Project BG051PO001/3.3-05-0001 "Science and Business", "Human Resources Development" Operational Programme co-financed by the European Social Fund of the EU and Bulgarian national budget. We wish to thank Dr R.M. Wilson at Queen Mary University of London for his help in X-ray data collection.*

REFERENCES

1. K. Mitzushima, P.C. Jones, P.J. Wiseman, J.B. Goodenough, *Mater. Res. Bull*., **15**, 783 (1980).
2. S.-K. Kim, W.-T. Jeong, H.-K. Lee, J. Shim, *Int. J. Electrochem. Sci*., **3**, 1504 (2008).
3. M.M. Thackeray, W.I.F. David, P.G. Bruce, J.B. Goodenough, *Mater. Res. Bull*., **18**, 461 (1983).
4. A.K. Padhi, K.S. Nanjundaswamy, J.B. Goodenough, *J. Electrochem. Soc*., **144**,1188 (1997).
5. J. Barker, M. Y. Saidi, Valence Technology Inc., US Patent 5,871,866 (1999).
6. Z. Bakenov, I. Taniguchi, *Electrochem. Commun*., **12**, 75 (2010).
7. K. Amine, H. Yasuda, M. Yamachi, *Electrochem. Solid-State Lett*., **3**, 178 (2000).
8. J. Wolfenstine, J. Allen, *J. Power Sources*, **142**,389 (2005).
9. J. Barker, R.K.B. Gover, P. Burns, A. Bryan, M.Y. Saidi, J.L. Swoyer, *J. Power Sources*, **146**, 516 (2005).
10. K. Rissouli, K. Benkhouja, J.R. Ramos-Barrado, C. Julien, *Mater, Sci. Eng. B***, 98**,185 (2003).
11. D. Morgan, A. Van der Ven, G. Ceder, *Electrochem. Solid State Lett*., **7**, A30 (2004).
12. L. Wang, Z.Tang, L. Ma, X. Zhang, *Electrochem. Commun*., **13**,1233 (2011).
13. Y. Li, L. Hong, J. Sun, F. Wu, S. Chen, *Electrochim. Acta*,, **85**,110 (2012).
14. Y. Lan, X. Wang, J. Zhang, J. Zhang, Z. Wu, Z. Zhang, *Powder Technol*., **212**, 327 (2011)
15. M.Y. Saïdi, J. Barker, H. Huang, J.L. Swoyer, G. Adamson, *J. Power Sources*, **119–121**, 266 (2003).
16. A. Tang, X. Wang, Z. Liu, *Mater. Lett*., **62**, 1646 (2008)
17. Y.-Z. Li, Z. Zhou, M.-M. Ren, X.-P. Gao, J. Yan, *Mater. Lett*., **61**, 4562 (2007).
18. Y. Chen, Y. Zhao, X. An, J. Liu, Y. Dong, L. Chen, *Electrochim. Acta*, **54**, 5844 (2009).
19. W. Yuan, J. Yan, Z. Tang, O. Sha, J. Wang, W. Mao, L. Ma, *Electrochimica Acta*, **72**, 138 (2012).
20. S. Zhong, L. Liu, J. Jiang, Y. Li, J. Wang, J. Liu, Y. Li, *J. Rare Earths*, **27**, 134 (2009).
21. J.N. Son, S.H. Kim, M.C. Kim, G.J. Kim, V. Aravindan, Y.G. Lee, Y.S. Lee, *Electrochim. Acta*,, **97**, 210 (2013)
22. R. Boukoureshtlieva, S. Hristov, J. Milusheva, A. Kaisheva, *Bulg. Chem. Commun*., **38**, 213(2006).
23. A. C. Larson, R. B. Von Dreele, *Los Alamos National Laboratory Report*, No. LAUR-86-748, (1987).
24. S.-C. Yin, H. Grondey, P. Strobel, M. Anne, L.F. Nazar, *J.Am. Chem. Soc*., **125**, 10402 (2003).
25. O.V. Yakubovich, V.S.Urusov, *Kristallografiya*, **42**, 301 (1997). (*In Russian*)
26. R.E. Loehman, C.N.R. Rao, J.M. Honig, *J. Phys. Chem*., **73**, 1781 (1969).
27. R.D. Shannon, *Acta Crystallogr. A***, 32**, 751 (1976).

СИНТЕЗ И ОХАРАКТЕРИЗИРАНЕ НА ЛИТИЕВО ВАНАДИЕВ ФОСФАТ, ДОТИРАН СЪС СИЛИЦИЙ И МАГНЕЗИЙ

С. М. Станков[1*], А. Момчилов[1], И. Абрахамс[2], И. Попов[1], Т. Станкулов[1], А. Трифонова[3]

[1] *Институт по електрохимия и енергийни системи „Акад. Евгени Будевски“ – Българска академия на науките, ул. „Акад. Г. Бончев“ бл. 10, София 1113, България*

[2] *Изследователски институт по материалиУчилище по биологически и химически науки,Университет „Кралица Мери”,Майл енд роуд,Лондон E1 4NS, Великобритания.*

[3] *AIT Австрийски институт за технологии, GmbH, Giefinggasse 2, 1210 Виена, Австрия.*

Постъпила на 12 май, 2014 г., коригирана на 15 юли, 2014 г.

(Резюме)

Активни материали за литиево-йонни батерии, базирани на дотиран с Si и Mg литиево ванадиев фосфат, $Li_3V_2(PO_4)_3$ (LVP), бяха синтезирани и изследвани чрез рентгеноструктурен, термогравиметричен и диференциално термичен анализи, трансмисионна електронна спектроскопия, галваностатични тестове и циклична волтамперометрия. $Li_3V_2(PO_4)_3$, $Li_{3.1}V_2(SiO_4)_{0.1}(PO_4)_{2.9}$, $Li_{3.5}V_2(SiO_4)_{0.5}(PO_4)_{2.5}$ и $Li_{3.04}Mg_{0.03}V_2(SiO_4)_{0.1}(PO_4)_{2.9}$ бяха получени чрез зол-гел метод, последван от твърдофазен синтез в аргонова атмосфера. Рентгеноструктурните анализи потвърдиха, че основната моноклинна кристалографска структура на LVP е запазена при дотираните съединения. Електрохимичните тестове, проведени в двуелектродни клетки, при токов режим 0.2C и диапазон от потенциали 2.8-4.4 V срещу Li/Li^+, показаха, че съединението, дотирано с Mg и Si отдава най-голям капацитет от 124.8 mA h g^{-1}, достигайки 94% от теоретичния си капацитет (133 mA h g^{-1}) в този интервал от потенциали. Въпреки това, този материал показва лошо поведение при циклиране, като загубата на капацитет е около 20% за направени 100 цикъла. Като цяло бе установено, че дотирането със силиций има неблагоприятно влияние върху електрохимичното поведение, но след първоначалния спад на капацитета от около 15% в първите 15 цикъла, двата материала, дотирани само със силиций, показаха относителна стабилност в последващите цикли.